Upper Bounds on Coarsening Rates in Demixing Binary Viscous Liquids

Yann Brenier, Felix Otto, Christian Seis

no. 460

Diese Arbeit ist mit Unterstützung des von der Deutschen Forschungsgemeinschaft getragenen Sonderforschungsbereichs 611 an der Universität Bonn entstanden und als Manuskript vervielfältigt worden.

Bonn, Oktober 2009

Upper bounds on coarsening rates in demixing binary viscous liquids

Yann Brenier*, Felix Otto†, and Christian Seis†

October 23, 2009

Abstract

We consider the demixing process of a binary mixture of two liquids after a temperature quench. Thermodynamics favors two domains of the two different equilibrium volume fractions with a characteristic interfacial layer. After an initial stage, the dynamics are thus driven by the reduction of the interfacial area. Therefore in large systems, one observes an increase in the typical length scale ℓ of the domains as a function of time t, a phenomenon called coarsening. In an intermediate stage, coarsening is mediated by cross-diffusion of the two species ("evaporation-recondensation process"). Siggia [21] argued that at a later stage, coarsening should be mediated by viscous flow of the mixture. Simple scaling arguments based on the assumption of statistical self-similarity of the domain morphology in time show that this hypothesis leads to a crossover in the coarsening rate: from $\ell \sim t^{1/3}$ for diffusion-mediated to $\ell \sim t$ for flow-mediated.

We consider a simple sharp-interface model which just allows for flow-mediated coarsening. For this model, we prove rigorously that coarsening cannot proceed faster than $\ell \sim t$ — without assumption of statistical self-similarity. The analysis follows closely a method proposed in [15], which is based on the gradient flow structure of the evolution. This method translates bounds on the energy landscape into bounds on the dynamics. The bounds on the energy landscape relate the energy functional (given by the driving thermodynamics — here interfacial energy) to the intrinsic distance in configuration space (determined by the limiting dissipation mechanism — here viscous dissipation). As opposed to the diffusion-mediated case, the intrinsic distance is not known explicitly; instead, we use a Monge-Kantorowicz-Rubinstein transportation distance with logarithmic cost functional as a proxy.

*CNRS, Université de Nice (FR 2800 W. Döblin), Institut Universitaire de France
†Institute of Applied Mathematics, University of Bonn, 53115 Bonn, Germany

1 Introduction

1.1 Background from physics

A view in the physicists' literature reveals a remarkable experimental and theoretical activity in the field of demixing processes of binary fluid mixtures. When a single phase system is suddenly placed into thermodynamically unstable two-phase state, e. g. by quenching from a high to a sufficiently low temperature, the phases separate by forming domains of the two different equilibrium volume fractions. The domain morphology coarsens with time: larger domains grow at the expense of smaller ones. The dynamics are driven by the free energy of the system. We refer to the review article [3] or the monograph [20].

The demixing proceeds in several stages. The initial stage, i. e., the formation of the domains with characteristic interfacial layers, is from the practical point of view negligible. With the exception of some very slowly diffusing systems, like polymer blends, the initial stage appears to be a short-time phenomenon — sometimes even to short to be easily observed.

The main focus of research is on the interfacial dynamics. When the domains are formed, the free energy of the system is concentrated on the interfaces. Since the system tries to minimize the energy, the amount of interfacial area decreases with time. This is realized by coarsening of the domain distribution. The characteristic length scale of the system, which describes the typical size of the domains, increases. In the interfacial dynamics two interesting features are numerically and experimentally observed: the morphology behaves statistically self-similar in time, and the growth rate of the characteristic length scale obeys a temporal power law.

The power-law exponent is determined by the growth mechanism within the demixing process. It can be heuristically derived by dimensional analysis based on the assumption of statistical self-similarity, cf. Subsection 1.5.

Siggia [21] studied the demixing process of binary viscous liquids at the critical concentration where both phases occupy the equal volume fraction. The physical growth mechanism is material transport from domains with high curvature to domains with low curvature. It originates from chemical potential differences. In the beginning of the interfacial dynamics, the material transport is mediated by cross-diffusion of the two phases ("evaporation-recondensation"). The coarsening rate is $\ell(t) \sim t^{1/3}$, when ℓ and t denote typical domain-size and time, respectively.

In viscous liquids mass is transported by convection as well as diffusion. Transport by convection can be much faster than transport by diffusion and it becomes dominant in later stages of coarsening. Based on simple scaling arguments on the relevant physical quantities Siggia predicted a crossover from $\ell(t) \sim t^{1/3}$ to $\ell(t) \sim t$ when the typical domain has achieved a certain size. Siggia's linear growth law has been confirmed by experiments, e. g. [27, 28, 5], and by numerical simulations, e. g. [19, 24, 14, 1].

Furthermore, there are two phenomena which may play a role in the very late stages of coarsening: gravity and inertia. Siggia remarked that for very large domains the growth rate undergoes a second crossover due to gravity and the density difference of the two coexisting phases [21, see e.g. p. 603]. The growth rate in this situation does not follow a power law and diverges in a finite time. On the other hand, Furukawa pointed out that the convective coarsening regime is limited by inertial effects. He predicted a inertial regime in which the typical domain size increases as $\ell(t) \sim t^{2/3}$, cf. [3, p. 375]. However, both effects does not seem to be of experimental relevance. We neglect these effects in our theoretical work.

In this paper we turn to Siggia's growth law for late stages of coarsening in binary viscous liquids. We derive a rigorous time-averaged upper bound on the coarsening rate $\ell(t) \sim t$. This bound is independent of the assumption of statistical self-similarity.

1.2 Background from mathematics

Mathematically, we follow closely a method proposed in [15], which relies on the gradient flow structure of the dynamics. Within the gradient flow structure, the functional encodes the driving energetics and the metric tensor the limiting dissipation mechanisms.

This point of view allows to translate

- bounds on the energy landscape, i. e., information on how fast the energy decreases as a function of (induced) *distance* to some reference configuration into
- bounds on the dynamics, i. e., bounds on how fast the energy decreases as a function of *time*.

Since a suitably renormalized Ginzburg-Landau-type free energy density has dimensions 1/length (it is proportional to the interfacial area per system volume) heuristically at least, lower bounds on the energy of some configuration translate into upper bounds on some average length scale of this configuration. If as expected, there is only one characteristic length scale present in the domain distribution, this is the relevant average length.

Note that upper bounds on coarsening rates are quite different from lower bounds. Upper bounds are universal, while lower bounds depend strongly on the geometry of the initial data. In fact, there exist configurations that do not coarsen at all (e. g. parallel planar layers).

The method in [15] is based on three ingredients:

- a statement on the energy density, more precisely, a lower bound of the energy in terms to the intrinsic distance (i. e., the distance induced by the metric

tensor coming from the dissipation mechanism) to some suitable reference configuration. Mathematically this typically amounts to an interpolation inequality.

- In certain cases, the intrinsic distance is not explicitly known (as in our case). In these situations, one has to identify a suitable explicit proxy to the intrinsic distance — and prove that it is bounded by the intrinsic distance.

- an ODE-argument.

It is crucial that all involved estimates are independent of the system size (for large system sizes).

The method proposed in [15] is quite robust. In the following, we try to give a short report on its applications.

- In the original paper [15], this approach was applied to the Cahn-Hilliard equation with constant and with degenerate mobility. Both equations model demixing of a binary mixture mediated by diffusion. In the constant mobility case, diffusion takes place in the bulk (i. e. the interior of the domains); whereas in the degenerate mobility case, diffusion only takes place along the interfacial layer. Physically, the constant mobility case corresponds to a shallow quench (i. e. temperature slightly below the critical temperature) whereas the degenerate mobility case corresponds to a deep quench (i. e. temperature much below the critical temperature). The Cahn-Hilliard equation with constant mobility is the gradient flow of a Ginzburg-Landau-type energy w. r. t. to the H^{-1}-inner product (i. e. a Euclidean situation), so that the induced distance is given by the H^{-1}-norm. The Cahn-Hilliard equation with degenerate mobility is the gradient flow of a Ginzburg-Landau-type energy w. r. t. to a weighted H^{-1}-inner product, which penalizes everything outside the interfacial layer (and thus is genuinely Riemannian). In order to treat both equations simultaneously, the Monge-Kantorowicz distance (i. e., the Monge-Kantorowicz-Rubinstein (MKR) distance with cost functional given by the Euclidean distance) was used as a proxy. In case of constant mobility, the authors of [15] obtain $E \gtrsim t^{-1/3}$; in case of degenerate mobility, they obtain $E \gtrsim t^{-1/4}$ — both exponents agree with the heuristics.

- The case of more than two components, both in the constant and degenerate mobility case, was treated in [17], with the same results.

- In [22], a generalized Cahn-Hilliard equation is investigated. The modifications are twofold: 1) The square gradient term in the Ginzburg-Landau energy functional is replaced by a non-local approximation (in fact, in the derivation of the Cahn-Hilliard equation as a mean-field model for Kawasaki dynamics in an Ising model with long-range interactions, this non-local attractive term arises in an intermediate step). 2) The constant mobility is replaced by a possibly

degenerate mobility. Under these modifications, the author establishes the same lower bound $E \gtrsim t^{-1/3}$ as for constant-mobility Cahn-Hilliard. Depending on the mobility, he uses two different proxies for the induced metric: The H^{-1}-norm and the Wasserstein distance (i. e., the MKR-distance with cost functional given by the square of the Euclidean distance).

- In [6], the case of an off-critical mixture in the constant mobility Cahn-Hilliard equation was treated. This means that the volume fraction Φ of one of the two phases is very small, and the corresponding domains come in form of small, distant, nearly immobile and nearly spherical particles. The configuration coarsens by "Ostwald ripening", which denotes the growth of the large particles at the expense of the small ones, which eventually vanish. Based on $\Phi \ll 1$, one can derive a reduced model that predicts the evolution of the distribution function $f(R)\,dR$ of particle radii, the celebrated Lifshitz-Slyozov-Wagner (LSW) theory. LSW theory heuristically predicts not just the scaling of the energy E in t, but also in the volume fraction $\Phi \ll 1$. It is given by $E \sim \Phi t^{-1/3}$ in the case of dimensions $d > 2$ and by $E \sim \Phi(\ln^{-1/3} \frac{1}{\Phi}) t^{-1/3}$ in the case $d = 2$. In this paper, these scalings are recovered as a lower bound. Here, the H^{-1}-inner product is used. Starting point is not Cahn-Hilliard, but its sharp interface version, known as Mullins-Sekerka in the mathematical literature.

- In [8], the starting point is now the LSW theory (see above), which mathematically speaking, is an evolution equation for the distribution function $f(R)\,dR$ of particle radii. Not surprisingly, it inherits the gradient flow structure of the original Cahn-Hilliard-type or phase-field model respectively their sharp-interface counterparts (i. e. variants of the Mullins-Sekerka or Stefan problems). The authors investigate the LSW theory of a Mullins-Sekerka model with kinetic undercooling (i. e. a convex combination of Mullins-Sekerka and mean-curvature flow). In case of dominant kinetic undercooling, they obtain the bound to be expected for mean curvature flow, i. e. $E \gtrsim t^{-1/2}$; in all other cases, they obtain $E \gtrsim t^{-1/3}$.

- In [9], the authors start not from the Cahn-Hilliard model with constant mobility but from a phase-field model. Heuristically, both models should have the same late stage behavior, as both give rise to the Mullins-Sekerka sharp interface motion. Indeed, the authors rigorously establish $E \gtrsim t^{-1/3}$. However, their analysis requires the domain size to be not too small compared to the system size.

- In [16], the authors treat a model from epitaxial growth; it models the evolution of the height $h(t, x)$ of a crystalline film on top of a substrate. The evolution is driven by an energy which favors slopes ∇h with $|\nabla h|^2 = 1$ but penalizes curvature $|D^2 h|^2$; it is limited by attachment kinetics. Mathematically speaking, this amounts to the L^2-gradient flow of a Ginzburg-Landau

energy in the vector-valued order parameter ∇h. Therefore, loosely speaking, it leads to a Cahn-Hilliard-type equation on the level of ∇h and thus one expects $E \sim t^{-1/3}$. This is proved as a lower bound. In view of the above discussion, the induced distance the authors use is the L^2-distance $\left(\int |h|^2 dx\right)$ to the flat surface. As opposed to the regular Cahn-Hilliard model, the set of favored order parameter values is not discrete. Therefore, the interpolation inequality is more subtle; the authors establish it via an indirect argument.

- In [18], the authors consider a model for viscous thin films. The evolution of the film height $h(t,x)$ is driven by the surface energy between liquid and vapor and a short-range attractive force between liquid and substrate; the latter leads to a precursor film of height normalized to unity. A typical configuration consists of equilibrium droplets with a contact angle normalized to $\frac{\pi}{4}$ sitting on top of the precursor film. Such a configuration coarsens by Ostwald ripening (see above). Asymptotic analysis [13] predicts the coarsening rate on a one-dimensional substrate ($d = 1$). In [18], the lower bound for the energy $E \geq t^{-\frac{d}{3d+2}}$ is proved. This lower bound coincides with the asymptotic analysis for $d = 1$ and is also conjectured to be optimal (up to a logarithm) for $d = 2$. However, this bound obtained by the [15]-method gives a suboptimal exponent for $d > 2$. This suboptimality is due to the same reason for which $E \gtrsim t^{1/3}$ is suboptimal for Cahn-Hilliard in $d = 1$: The [15]-method relies on a very coarse property of the energy landscape, which is too coarse for the plateau and step structure of the energy landscape of the Cahn-Hilliard equation in $d = 1$.

  Mathematically speaking, the model in [18] is similar to the Cahn-Hilliard equation with two modifications: 1) In the Ginzburg-Landau model, the usual symmetric double well potential $W(h)$ is replaced by a nonlinearity $W(h)$ with one well at $h = 1$ and the other well at $h = +\infty$. 2) The constant mobility in the Cahn-Hilliard equation is replaced by a linear mobility h. In this situation, the induced distance is no longer the H^{-1}-norm but the Wasserstein distance. The reason for the dimension-dependent coarsening exponent lies in the fact that energetically, the model is $d+1$-dimensional (droplets in form of $d+1$-dimensional parabola caps), whereas from the point of view of dissipation, the model is d-dimensional (diffusion through the d-dimensional precursor layer).

- In [10], the authors consider a discrete version of the Cahn-Hilliard equation, where the discrete nature replaces the regularizing effect of the fourth-order term. In one space dimension, this model relates to the Perona-Malik model in image denoising. This model is the gradient flow of a non-convex functional (convex at $m = 0$ but non-convex for $m \uparrow \infty$, favoring $m = 0$ and spikes $m = \infty$) with respect to a discrete version of the H^{-1}-inner product. The authors obtain the same lower bound on the energy as in the continuum case. In [11], the authors consider a more general class of non-convex functionals classified by an exponent α for large m-values. They find optimal lower bounds on the energy with an exponent which depends on α.

In our analysis, we adopt the method from [15] to a simple sharp-interface model for flow-mediated coarsening. This means that the driving energy functional is the surface energy of the configuration $m \in \{-1, 1\}$ and the limiting dissipation mechanism is the viscous dissipation of the incompressible velocity u which convects m. For this dissipation mechanism, the genuinely Riemannian distance is not known explicitly. We use a Monge-Kantorowicz-Rubinstein (MKR) distance as a proxy for this induced distance to the "microscopically mixed state" $m \equiv 0$. This MKR-distance has to be chosen in such a way that it is dominated by this induced distance given by the viscous dissipation mechanism, i. e. $\int |Du|^2 \, dx$. Since the dissipation mechanism only controls the *gradient* of the convecting velocity, it is not surprising that the cost functional in the MRK-distance can only grow logarithmically. The fact that the MRK-distance indeed is dominated is connected to a conjecture of Bressan [4, p. 4], see also [7, p. 25]. In the L^p-setting ($p > 1$) instead of the L^1-setting considered in [4], this conjecture was solved in [7], which in turn can be understood as a quantification of the DiPerna-Lions theory of renormalizable solutions to convection equations. In a certain sense, in this paper we reformulate the result in [7] in terms of our MRK-distance.

The paper is organized as follows. In Subsection 1.3 we describe the full model for demixing processes in binary viscous liquids involving the Ginzburg-Landau energy from which our simple sharp-interface model can be derived. In Subsection 1.4 we provide a gradient flow interpretation of the full model. We argue heuristically in favor of the predicted scaling law in Subsection 1.5. Subsection 1.6 presents our numerical simulations. Section 2 provides our analytic results in the sharp-interface model. Finally, Section 3 contains the proofs. We attach two appendices for technical convenience.

1.3 The full model

We are interested in the late-stage coarsening phenomenon which occurs when a thermodynamically unstable two-phase system, in our case a binary viscous liquid quenched slightly below a critical temperature, demixes, i. e., the two phases separate into two domains of the two different equilibrium volume fractions. As order parameter, which locally describes the composition of the mixture at any one time, we consider a scalar field

$$m(t, x) \in \mathbb{R}.$$

The free energy is given by the Ginzburg-Landau functional

$$E(m) \;=\; \int \frac{1}{2}|\nabla m|^2 + \frac{1}{2}(1 - m^2)^2 \, dx, \tag{1}$$

which favors locally the separation of the system into its two phases, encoded by the values -1 and 1, and penalizes transitions between domains occupied by different phases. Hence length, energy, and order parameter have been nondimensionalized

such that the equilibrium values, the width of the interfacial layers, and the energy per area of the interfacial layers are all of order one. Furthermore, we have normalized the free energy by the volume of the system, denoting the average by $⨍ dx$.

The evolution must conserve the volume fraction of each phase separately. We are interested in the case of a "critical mixture", where both phases occupy the same volume fraction, i. e.,

$$⨍ m\,dx \;=\; 0. \tag{2}$$

This leads to a conservation law for m:

$$\partial_t\, m + \nabla\cdot J \;=\; 0,$$

for some flux J. The flux takes account of the two parallel transport mechanisms: diffusion and convection. Diffusion is the relative motion of the unlike particles. In liquids, it originates from chemical potential differences. The diffusive flux J_{diff} is therefore given by $J_{diff} = -\lambda\nabla\mu$, where λ is the diffusion coefficient and μ is the chemical potential, which is defined by

$$\mu \;=\; \frac{\partial E}{\partial m} \;=\; -\Delta m - 2(1-m^2)m.$$

Convection is the flow of the bulk with a velocity field u. The convective flux J_{conv} is therefore given by $J_{conv} = m\,u$.

We may recapitulate the evolution equation:

$$\partial_t\, m - \lambda\Delta\mu + \nabla\cdot(m\,u) \;=\; 0. \tag{3}$$

We want to relate the velocity u of the bulk flow to the thermodynamic driving forces: the velocity obeys a Stokes equation

$$-\eta\Delta u + \nabla p \;=\; -m\nabla\mu, \tag{4}$$

$$\nabla\cdot u \;=\; 0, \tag{5}$$

where η is the viscosity coefficient and p is the pressure. The liquid is incompressible, equation (5). The r. h. s. of (4) arises from the energy change that accompanies the liquid transport ("principle of virtual work"): the gradient of the chemical potential acts as a driving force on the liquid. Note that $m\nabla\mu$ equals to $\nabla\cdot(\nabla m\otimes\nabla m)$ up to terms that can be absorbed in the pressure gradient.

We use the Stokes approximation of the Navier-Stokes equation by neglecting the inertial terms. This amounts to the assumption that the flow velocity responds nearly instantaneously to changes of the order parameter. The velocity is then "slaved to the order parameter". In fact, this approximation fails for very large domains. We will neglect these inertia influences in our setting. See also [3, p. 374-376] for a precise determination of the different scaling regimes.

We may absorb one of the dimension free parameters in the time scale: for convenience we set $\eta = 1$.

1.4 The gradient flow structure

We like to embed our model into an abstract framework, at least heuristically. We interpret the system (3, 4, 5) as a gradient flow, i. e., the evolution follows the steepest descent in an energy landscape. Mathematically, this requires a differentiable manifold $\mathcal{M}$, together with a metric tensor g, and an energy functional E on $\mathcal{M}$. The dynamical system in $\mathcal{M}$ given by the differential equation

$$\partial_t m + \operatorname{grad} E_{|m} \;=\; 0 \tag{6}$$

is called the gradient flow of E on $(\mathcal{M}, g)$. The energy gradient $\operatorname{grad} E$ is related to the differential $\operatorname{diff} E$ of E by the Riesz representation theorem:

$$g_m(\operatorname{grad} E, \delta m) \;=\; \operatorname{diff} E.\,\delta m \qquad \text{for all tangent vectors } \delta m \text{ at } m.$$

This allows for the gradient free reformulation of (6):

$$g_m(\partial_t m, \delta m) + \operatorname{diff} E_{|m}.\,\delta m \;=\; 0 \qquad \text{for all tangent vectors } \delta m \text{ at } m, \tag{7}$$

or equivalently, coming from the variational point of view,

$$\partial_t m \;=\; \arg\min_{\delta m} \left\{ \tfrac{1}{2}\, g_m(\delta m, \delta m) + \operatorname{diff} E_{|m}.\,\delta m \;\middle|\; \delta m \text{ tangent vector at } m \right\}. \tag{8}$$

For the gradient flow interpretation of the dynamic system (3, 4, 5) we still have to identify the ingredients $\mathcal{M}$ and g. The energy functional reflects the driving energetics. It is given by the initially introduced Ginzburg-Landau functional (1).

The evolution must conserve the order parameter. For simplicity we consider the case of equal volume fraction, (2). Accordingly, the manifold is given by

$$\mathcal{M} \;=\; \left\{ m \text{ with } \fint m\,dx \;=\; 0 \right\}. \tag{9}$$

The metric tensor g encodes the limiting dissipation mechanisms. Choosing the admissible tangent vector $\partial_t m$ in the gradient flow notion (7), we find:

$$\frac{d}{dt} E(m) \;=\; \operatorname{diff} E_{|m}.\,\partial_t m \;=\; -g_m(\partial_t m, \partial_t m).$$

Two different dissipation mechanisms due to diffusion and convection occur in the demixing of binary liquids: dissipation by friction as a result of collisions of particles ("outer friction") and dissipation by friction because of viscosity (Stokes friction or "inner friction"). This suggests to choose the metric tensor as

$$\begin{aligned} &g_m(\delta m, \delta m) \\ &\quad= \inf_{(u,\,j)} \left\{ \fint \lambda |j|^2 + \tfrac{1}{2} |(Du + (Du)^t)|^2 \, dx \;\middle|\; \delta m + \lambda \nabla\cdot j + \nabla\cdot(mu) = 0,\ \nabla\cdot u = 0 \right\} \\ &\quad= \inf_{(u,\,j)} \left\{ \fint \lambda |j|^2 + |Du|^2 \, dx \;\middle|\; \delta m + \lambda \nabla\cdot j + \nabla\cdot(mu) = 0,\ \nabla\cdot u = 0 \right\}. \end{aligned} \tag{10}$$

Thus the minimization problem (8) can be written, using Lagrange multipliers:

$$\inf_{(\delta m,u,j)} \sup_{(\phi,p)} \left\{ \int \frac{\lambda|j|^2 + |Du|^2}{2} - (\lambda j + mu) \cdot \nabla\phi + \phi\,\delta m + \nabla p \cdot u + \frac{\partial E}{\partial m}\delta m\,dx \right\},$$

which easily leads to the optimality conditions. We immediately recover:

$$\phi = -\frac{\partial E}{\partial m},\ j = \nabla\phi,\ -\Delta u + \nabla p = m\nabla\phi.$$

1.5 Heuristics

Physical experiments and numerical simulations suggest that the coarsening rate of the domain pattern shows a simple behavior (cf. Section 1.6). In sufficiently large systems and it can be described by a power law:

$$\ell(t) \sim t^\gamma,$$

for $t \gg 1$. We are interested in understanding the mechanisms which determine the dynamic exponent γ. In this section, we derive γ by heuristical considerations, which are based on the (unproven) statistical self-similarity.

In binary liquids, demixing mediates by diffusion and convection. To determine the contribution of each transport mechanism to the growth of the characteristic length scale, we consider both mechanisms separately.

We study the mesoscopic version of the model. Inside of the domains, the order parameter is nearly uniform, $m \approx \pm 1$. It varies with a characteristic interfacial layer along the interface between the domains. For this reason, the energy contribution in the bulk is negligible. The energy is concentrated on the interface between the domains. Therefore, we approximate

$$\begin{aligned} \text{energy} \ &\approx\ \text{energy of 1-d interfacial layer} \\ &\quad \times \text{area of sharp interface per system volume.} \end{aligned}$$

A simple calculation shows that the energy of the one-dimensional layer is 4/3. The above approximation motivates the mesoscopic version of the model. Assuming the interface to be sharp, $m = \pm 1$, an appropriate energy is given by

$$E(m) \ = \ \frac{4}{3} \times \frac{1}{2} \int |\nabla m|\,dx \ = \ \frac{2}{3} \int |\nabla m|\,dx.$$

Here we have used the convenient geometric measure theory notation. Moreover, we write $\Omega = \{m = \pm 1\}$ for the bulk, and $\Gamma = \partial\Omega$ for the interface.

We assume the validity of the gradient flow structure for the sharp-interface model. In order to derive the classical equations for the evolution, we consider the variational formulation of the gradient flow (8). Variations of the order parameter correspond to variations of the interface. We measure such variations infinitesimally by a normal

velocity $2V$ along Γ. (Notice that $\partial_t m = 2V|\nabla m|$.) An infinitesimal variation of the energy is given by $\frac{4}{3}\fint HV\, d\mathcal{H}^{d-1}\llcorner\Gamma$, where H denotes the mean curvature of Γ.

In the purely diffusive regime, the only dissipative mechanism is outer friction. According to (8) we thus have to identify

$$\arg\min_V \left\{ \tfrac{1}{2} \min_j \left\{ \fint \lambda |j|^2 \, dx \,\middle|\, \nabla\cdot j = 0 \text{ in } \Omega,\ \lambda[\nu\cdot j] = 2V \text{ on } \Gamma \right\} + \tfrac{4}{3} \fint HV \, d\mathcal{H}^{d-1}\llcorner\Gamma \right\},$$

where where ν denotes a normal on Γ, and $[.]$ denotes the jump across Γ. On the level of j:

$$\arg\min_j \left\{ \tfrac{1}{2} \fint \lambda |j|^2 \, dx + \tfrac{2}{3} \fint H\lambda[\nu\cdot j] \, d\mathcal{H}^{d-1}\llcorner\Gamma \,\middle|\, \nabla\cdot j = 0 \text{ in } \Omega \right\}.$$

A computation of the Euler-Lagrange equation gives the well-known Mullins-Sekerka evolution equations:

$$-\Delta\mu \;=\; 0,$$

in the bulk Ω, and

$$\begin{aligned} \mu &= \tfrac{2}{3}H, \\ 2V &= -\lambda[\nu\cdot\nabla\mu], \end{aligned}$$

on the interface Γ. This amounts to a third order free boundary value problem. Hence the solution space is invariant under rescaling

$$x \longrightarrow \sigma\, x, \quad t \longrightarrow \sigma^3\, t.$$

Consequently, if we assume the solution behaves statistically self-similar, the scaling exponent must be $1/3$. Indeed, m being statistically self-similar means

$$|\mathcal{F}m(t,\,\cdot\,)(k)|^2 \;\approx\; f(t^\gamma k),$$

for some structure function f and every wave number k. As usual, $\mathcal{F}m$ denotes the Fourier transform of m. By scaling invariance of the solution space, this turns into

$$f(t^\gamma k) \;\approx\; |\mathcal{F}m(\sigma^3 t, \sigma\cdot\,)(k)|^2 \;=\; |\mathcal{F}m(\sigma^3 t,\,\cdot\,)(\sigma^{-1}k)|^2.$$

Hence

$$f(t^\gamma k) \;\approx\; f((\sigma^3 t)^\gamma(\sigma^{-1}k)),$$

which yields $\gamma = 1/3$, since σ is arbitrary. Thus

$$\ell(t) \sim (\lambda t)^{1/3}.$$

Notice that in this reduced model, λ can be absorbed in the time scale. Therefore λ must have the same exponent as t in the coarsening rate.

In the purely convective regime, the dissipative mechanism is Stokes friction. Therefore we have to identify

$$\arg\min_V \left\{ \tfrac{1}{2} \min_u \left\{ \int |Du|^2 \, dx \,\middle|\, \nabla\cdot u = 0,\ \nu\cdot u = V \text{ on } \Gamma \right\} + \tfrac{4}{3} \int HV \, d\mathcal{H}^{d-1}\llcorner\Gamma \right\},$$

respectively

$$\arg\min_u \left\{ \tfrac{1}{2} \int |Du|^2 \, dx + \tfrac{4}{3} \int H\nu\cdot u \, d\mathcal{H}^{d-1}\llcorner\Gamma \,\middle|\, \nabla\cdot u = 0 \right\},$$

A computation of the Euler-Lagrange equations yields

$$\begin{aligned} \nabla\cdot u &= 0, \\ -\nabla\cdot S &= 0, \end{aligned}$$

in the bulk Ω, and

$$\begin{aligned} V &= \nu\cdot u, \\ \tau\cdot[S]\nu &= 0, \\ \nu\cdot[S]\nu &= -\tfrac{4}{3}H, \end{aligned}$$

on the interface Γ. Here $S = Du + (Du)^t - p\,\mathrm{id}$ denotes the stress tensor. The boundary value problem is of order one. Hence if the growth of the characteristic length scale behaves statistically self-similar, a similar calculation as above shows that the dynamic exponent must be one:

$$\ell(t) \sim t.$$

Comparing both scaling laws, diffusion-mediated coarsening proceeds much faster for $t \ll \lambda^{1/2}$, and flow-mediated coarsening proceeds much faster for $t \gg \lambda^{1/2}$. The coarsening rate is determined by the faster transport mechanism. Consequently, we expect a crossover at

$$t \sim \lambda^{1/2}$$

from a first, diffusion dominated regime to a second, convection dominated regime.

1.6 Numerical simulations

We present our numerical simulations for the demixing process in binary liquids in two space dimensions.

For our numerical simulations we use the full smooth-interface model (3, 4, 5) in two space dimensions with periodic boundary conditions. The system size is Λ. We treat the case $\lambda = 1$.

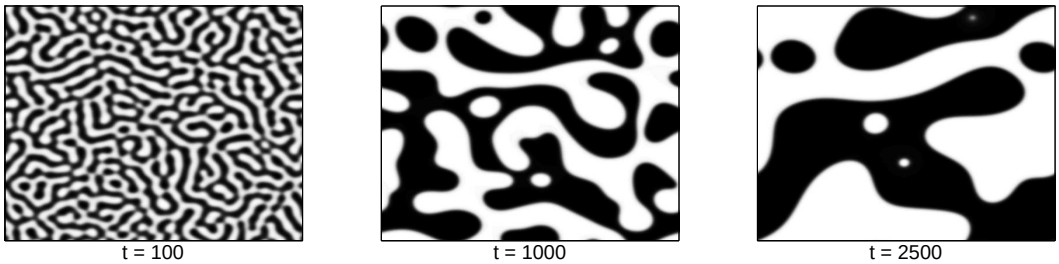

Figure 1: Plots of a numerically computed coarsening process in a binary viscous mixture.

We use a semi-implicit time discretization of the evolution equation (3), which is explicit in the nonlinear and in the convective term:

$$\left(\frac{1}{\Delta t} + \Delta^2 + 2\Delta\right) m^{k+1} \;=\; 2\Delta (m^k)^3 - \nabla\cdot(m^k u^k) + \frac{1}{\Delta t} m^k. \tag{11}$$

Exploiting the incompressibility condition (5), the velocity u^k is determined by two Poisson equations. If we denote the velocity components by v^k and w^k, these read

$$\begin{aligned} -\Delta v^k &= f^k - \partial_x \Delta^{-1}(\partial_x f^k + \partial_y g^k), \\ -\Delta w^k &= g^k - \partial_y \Delta^{-1}(\partial_x f^k + \partial_y g^k), \end{aligned}$$

where the forces f^k, g^k are given by

$$\begin{aligned} f^k &= \partial_x(\partial_x m^k \partial_x m^k) + \partial_y(\partial_x m^k \partial_y m^k), \\ g^k &= \partial_x(\partial_x m^k \partial_y m^k) + \partial_y(\partial_y m^k \partial_y m^k). \end{aligned}$$

We compute f^k, g^k, and the nonlinear term in (11) with the help of a finite difference scheme. For the convective term we apply the upwind method. Subsequently, the equations for v^k, w^k, and m^{k+1} are solved with FFT. As initial data we impose a white noise with amplitude 10^{-2} and mean value zero.

In this paper we present our numerical simulations for the system size $\Lambda = 50\,\pi$. Figure 1 shows three stages of a computed coarsening process for a binary viscous mixture. It turns out that $\Lambda = 50\,\pi$ is a system size for which the expected coarsening rate can be observed — at least in the very late stages and for a very short time (see below). On the other hand, using our simple implementation, $\Lambda = 50\,\pi$ appears to be near the upper limit of system sizes for which computations on a desktop computer can be realized within a reasonable running time.

Some experiences suggest that initially, the time step size should be chosen of order 10^{-4}. If the phases were separated and the domain morphology had become sufficiently coarse, we increased the time step size up to 10^{-3}. An optimal or even an adaptive choice of the time step size have not been worked out.

In Figure 2 we have plotted the energy evolution with a logarithmic axes scaling. In the very late stages it approaches "asymptotically" the slope -1. As motivated in the previous section, a crossover from $-1/3$ to -1 is expected at $t \sim \lambda^{1/2}$, and can therefore not be observed (since $\lambda = 1$ is too small). Instead, we find a continuously accelerating decrease of the energy density after an initial stage ($t \lessapprox 100$) of demixing.

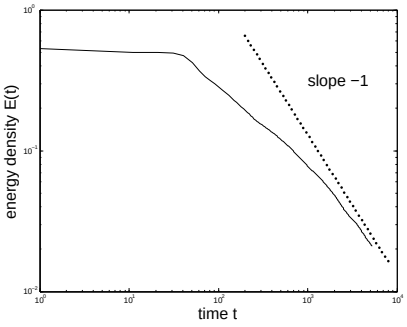

Figure 2: Energy density vs. time.

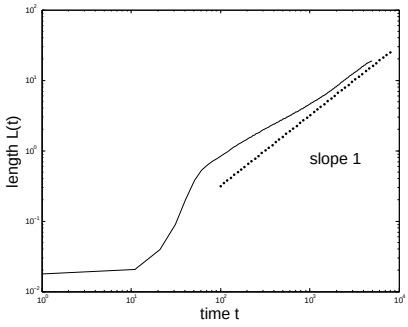

Figure 3: H^{-1}-norm vs. time.

In order to observe the predicted crossover, one has to choose a significant larger diffusion coefficient, such as a larger system size. However, as mentioned above, this cannot be realized within a reasonable running time.

Figure 3 shows the logarithmic plot of the "length" $L(t)$ vs. time. Here $L(t)$ is defined as the H^{-1}-norm of the order parameter:

$$L(t) \;=\; \left(\fint ||\nabla|^{-1} m|^2 \, dx \right)^{1/2} .$$

Because the H^{-1}-norm is the induced distance to the fully mixed configuration ($m \equiv 0$) in the gradient flow interpretation for diffusion-mediated coarsening, it can be considered as *a* natural length scale in our experiment. Since the intrinsic distance (i. e., the induced distance from the gradient flow interpretation) for the flow-mediated coarsening is not known explicitly, it is convenient to consider only this quantity as any measure of length. We observe that in the interfacial regime, the growth of $L(t)$ proceeds slightly slower than t. Furthermore, it seems to converge in the very late stages "asymptotically" to t.

2 Main results

Our analysis follows closely the method proposed in [15], which relies on the gradient flow structure of the dynamics. See Subsection 1.2 for discussion and references.

The procedure is the following. Since in our case the intrinsic distance is not known explicitly, we have to identify a suitable explicit proxy, which is bounded by the

intrinsic distance to some reference configuration. We derive an interpolation estimate involving proxy and energy, and use an ODE-argument to establish the upper bound on the coarsening rate.

We have motivated an appropriate mathematical formulation for the demixing process in binary viscous liquids in Subsection 1.3. However, for the sake of simplicity, we prefer to work on a mesoscopic level, as in Subsection 1.5. This means, we approximate the full model by its sharp-interface version. Furthermore, our model presented here only allows for flow-mediated coarsening. This corresponds to the case $\lambda = 0$. Anyhow, we believe that the results presented here are valid even in the full model, which we plan to address in a future paper.

On the mesoscopic level, the order parameter m takes the values ± 1. We restrict or attention to the case of a critical mixture, i. e.,

$$\fint m \, dx = 0,$$

equation (2). The energy contribution of the Ginzburg-Landau energy (1) concentrates on the interfacial layers between the domains. The energy assigned to the sharp-interface model is

$$E(m) = \fint |\nabla m| \, dx. \tag{12}$$

The metric tensor (10) reduces to

$$g_m(\delta m, \delta m) \;=\; \inf_u \left\{ \fint \frac{1}{2} |Du|^2 \, dx \;\middle|\; \delta m + \nabla \cdot (mu) = 0, \; \nabla \cdot u = 0 \right\}. \tag{13}$$

For the PDEs we impose periodic boundary conditions. All averages are taken over the period cell. The size Λ of the period cell is effectively the system size. Since we are always working with averages, the system size does not enter in our analysis. In particular, our results are independent of Λ.

For two configurations m_0, m_1, the distance induced by the metric tensor is given by

$$\operatorname{dist}(m_0, m_1) \;=\; \inf_{\tilde{m}} \left\{ \int_0^1 g_{\tilde{m}}(\partial_t \tilde{m}, \partial_t \tilde{m}) \, dt \;\middle|\; \tilde{m}(0) = m_0, \; \tilde{m}(1) = m_1 \right\}.$$

For g defined by (13) this distance is not known explicitly. We have to identify an appropriate proxy $D(m)$. The [15]-method is illustrated in the following proposition.

Proposition 1. *Let there be a function $D(m)$ such that*

$$|\operatorname{grad} D_{|m}|^2 \lesssim 1 \quad \textit{for any } m, \tag{14}$$

and

$$\ln E(m) \gtrsim -D(m) \quad \textit{for any } m \textit{ such that } E(m) \leq 1. \tag{15}$$

Then for any solution of

$$\partial_t\, m + \operatorname{grad} E_{|m} \;=\; 0 \tag{16}$$

with $E(0) \ll 1$ *we have*

$$\int_0^T E(m(t))\, dt \gtrsim \ln T \quad \textit{for any } T \textit{ such that } \ln T \gg D(m(0)).$$

Since the energy density has dimensions *1/length*, it can be considered as an inverse length scale. Assuming that there is only one length scale is present in the domain distribution, we can measure it by the inverse energy density. Consequently, a dynamic lower bound on the energy can be interpreted as an upper bound on the coarsening rate.

Notice that Proposition 1 treats the particular case $\alpha = \infty$, where α denotes the geometric exponent in the notation from [18, Prop. 1].

We do not claim the existence of a gradient flow structure

$$\partial_t\, m + \operatorname{grad} E(m) \;=\; 0,$$

equation (16), in any particular sense. Our diction is just symbolic but our treatment is fully rigorous in the end. Anyhow, in this paper, *we assume that a solution exists.* It can be a *weak solution* in the sense that we only need

- the transport equation $\partial_t\, m + \nabla \cdot (mu) = 0$ in a distributional sense,
- the incompressibility $\nabla \cdot u = 0$,
- the energy dissipation inequality $\frac{d}{dt} \fint |\nabla m| dx \le -\fint |Du|^2 dx$.

To our knowledge, it is open whether such a solution exists for all (suitable) initial data for all times. Since we plan to address the full model in a future paper, for which well-posedness is obvious, with similar methods, we believe that this lack of existence theory is acceptable.

The gradient notion in (14) is also only symbolic. What we mean is provided in Proposition 2 below. Finally, (15) is established in Proposition 3.

Now we want to specify our choice of $D(m)$. For any given order parameter $m \in [-1, 1]$ with (2), we define

$$\begin{aligned} &D(m) \\ &\quad= \inf \left\{ \fint\!\!\fint c(|x_1 - x_0|)\, d\pi(x_0, x_1) \,\middle|\, \int d\pi(\,.\,, x_1) = 1,\ \int d\pi(x_0,\,.\,) = m + 1 \right\}, \end{aligned} \tag{17}$$

where we continue writing $\fint\!\!\fint d\pi = \frac{1}{\Lambda^d} \iint d\pi$. Such Monge-Kantorowicz-Rubinstein distances are naturally domiciled in the field of optimal transportation. Informally, the cost function $c(z)$ measures the cost of mass transportation over a distance z,

and the transfer plan π encodes the way of transportation. Good references to this topic are Villani's books [25] and [26]. See also Appendix A.

To our aim, we use a logarithmic cost function $c(z) = \ln(z+1)$. With that choice we have the desired Lipschitz-property (14):

Proposition 2. *Let $c(z) = \ln(z+1)$. Let $m \in [-1,1]$ with $\int m\,dx = 0$ and u be related by*

$$\partial_t m + \nabla\cdot(mu) = 0, \tag{18}$$
$$\nabla\cdot u = 0. \tag{19}$$

Then we have for a. e. $t > 0$:

$$\frac{d^+}{dt} D(m(t)) \lesssim \left(\fint |Du(t,x)|^2\,dx \right)^{1/2}. \tag{20}$$

The transport equation (18) has to be read in the sense of distributions.

Assumption (15) in Proposition 1 can be established for a much larger class of Monge-Kantorowicz-Rubinstein distances. In fact, for arbitrary monotone increasing cost functions we have the following kind of interpolation inequality:

Proposition 3. *Let $c(z)$ be monotone increasing with $c(0) = 0$. Let $m \in \{-1,1\}$ with $\int m\,dx = 0$.*
Then there is an only d-dependent constant c_0 such that

$$D(m) \gtrsim c\left(\frac{1}{c_0 \fint |\nabla m|\,dx} \right). \tag{21}$$

As a corollary from the above propositions, we may state our main result.

Theorem 1. *Assume that $\partial_t m + \operatorname{grad} E_{|m} = 0$ and $E(0) \ll 1$. Then we have*

$$\int_0^T E(m(t))\,dt \gtrsim \ln T \qquad \text{for any } T \text{ such that } \ln T \gg D(m(0)).$$

The method in [15] only provides time-averaged upper bounds on coarsening rates. However, within this framework the pointwise statement,

$$E^{-1} \lesssim t,$$

cannot be derived. Counter-examples in this flavor are given in [15, Remark 4] or [18, Remark 2].

3 Proofs

We start with the proof of Proposition 2. The first part provides an estimate on the rate of change of $D(m)$ against a Lipschitz norm of u. It follows from Lemma 1 by an approximation argument.

The second part, the estimate of the Lipschitz norm of the convecting velocity field against a gradient norm, was inspired by the proof of [7, Theorem 2.1 resp. Theorem 3.3].

Proof of Proposition 2 As a first step, we derive an estimate on the rate of change of $D(m(t))$, more precisely,

$$\frac{d^+}{dt} D(m(t)) \;\leq\; \iint \frac{|u(t,x_1) - u(t,x_0)|}{|x_1 - x_0|}\, d\pi_{opt}(t)(x_0,x_1). \tag{22}$$

To this aim, we consider a regularization of u: Let u_ε denote the convolution with a standard mollifier, such that $\nabla\cdot u_\varepsilon = 0$ and u_ε approximates u in $L^1(W^{1,2}_{per})$ (this is the natural class for the transporting velocity field in our gradient flow formulation). We denote by m_ε the solution of the regularized transport equation

$$\partial_t\, m_\varepsilon + \nabla\cdot(u_\varepsilon m_\varepsilon) \;=\; 0, \tag{23}$$

in some time interval $[t, t+h]$, with initial data $m_\varepsilon(t,\,\cdot\,) = m(t,\,\cdot\,)$. Then $m_\varepsilon \in C([t,t+h]; L^2_{per}(0,\Lambda)^d))$ is of the form $m_\varepsilon(t+s, \phi_\varepsilon(s,x)) = m(t,x)$, for $s \in [0,h]$, when ϕ_ε denotes the flow of $u_\varepsilon(t+\cdot\,,\,\cdot\,)$, i. e. $\partial_s\phi_\varepsilon(s,x) = u_\varepsilon(t+s,\phi_\varepsilon(s,x))$ and $\phi_\varepsilon(0,x) = x$. In particular,

$$\frac{1}{h}\int_t^{t+h} \!\!\fint m_\varepsilon(s,x)^2\, dxds \;=\; \fint m(t,x)^2\, dx. \tag{24}$$

We are now in a position to apply Lemma 1 in Appendix A with $\rho_0 = m_\varepsilon + 1$ and $\rho_1 = 1$. We find the inequality:

$$\frac{d^+}{dt} D(m_\varepsilon(t)) \;\leq\; \iint c'(|x_1-x_0|)\frac{x_1-x_0}{|x_1-x_0|}\cdot(u_\varepsilon(t,x_1) - u_\varepsilon(t,x_0))\, d\pi_{\varepsilon,opt}(t)(x_0,x_1),$$

where $\pi_{\varepsilon,opt}$ denotes the optimal transfer plan. By the choice of c we get

$$\begin{aligned}\frac{d}{dt} D(m_\varepsilon(t)) \;&\leq\; \iint \frac{|u_\varepsilon(t,x_1) - u_\varepsilon(t,x_0)|}{|x_1-x_0|}\, d\pi_{\varepsilon,opt}(t)(x_0,x_1)\\ &\leq\; \iint \frac{|u(t,x_1) - u(t,x_0)|}{|x_1-x_0|}\, d\pi_{\varepsilon,opt}(t)(x_0,x_1).\end{aligned}$$

We need a compactness argument to deduce (22). From (24), we infer that m_ε converges weakly to some $\tilde m$ in L^2 in time-space (up to a subsequence). Notice that by the uniqueness result of the DiPerna-Lions theory for renormalized solutions, cf. [2, Theorem 4.2], $m = \tilde m$, so that we recover the solution (m,u) of the original problem (18) by passing to the limit in the distributional formulation of (23).

Integrating the above inequality over the time interval $[t, t+h]$ yields a convenient expression for the limit $\varepsilon \downarrow 0$:

$$D(m_\varepsilon(t+h)) - D(m_\varepsilon(t)) \;\le \int_t^{t+h} \!\!\!\!\!\!\iint \frac{|u(s,x_1) - u(s,x_0)|}{|x_1 - x_0|}\, d\pi_{\varepsilon,opt}(s)(x_0,x_1) ds.$$

We get by the lower semicontinuity of $D(m)$ with respect to weak L^2-convergence:

$$D(m(t+h)) - D(m(t)) \;\le \int_t^{t+h} \!\!\!\!\!\!\iint \frac{|u(s,x_1) - u(s,x_0)|}{|x_1 - x_0|}\, d\pi_{opt}(s)(x_0,x_1) ds.$$

Recall that $m_\varepsilon(t) = m(t)$. The convergence of the r.h.s. follows from the stability of the optimal transfer plans, cf. [26, Theorem 5.20], and the uniqueness of π_{opt}. We divide by h and find (22) in the limit $h \downarrow 0$.

Now we turn to (20). This part of the proof uses the notion of maximal functions, $(M f)(x_0) = \sup_{r>0} \frac{1}{|B_r|} \int_{B_r(x_0)} f\, dx$. We report that (see Lemma 2 in Appendix B)

$$|u(x_1) - u(x_0)| \;\lesssim\; |x_1 - x_0| \left((M\,|Du|)(x_1) + (M\,|Du|)(x_0) \right),$$

so that (22) turns to

$$\begin{aligned}
\frac{d^+}{dt} D(m(t)) \;&\lesssim\; \iint \left((M\,|Du|)(t,x_1) + (M\,|Du|)(t,x_0) \right) d\pi_{opt}(t)(x_0,x_1) \\
&=\; \fint (M\,|Du|)(t,x_1)(m+1)(t,x_1)\, dx_1 + \fint (M\,|Du|)(t,x_0)\, dx_0 \\
&\lesssim\; \left(\fint \left((M\,|Du|)(t,x) \right)^2 dx \right)^{1/2}.
\end{aligned}$$

Now we need the following property of the maximal function: For any $p \in (1,\infty)$ we have

$$\left(\int |M f|^p\, dx \right)^{1/p} \;\lesssim\; \left(\int |f|^p\, dx \right)^{1/p},$$

see Lemma 3 in Appendix B. This yields

$$\frac{d^+}{dt} D(m(t)) \;\lesssim\; \left(\fint |Du(t,x)|^2\, dx \right)^{1/2}. \tag{25}$$

□

We now turn to the proof of Proposition 3.

Proof of Proposition 3 Let π be an admissible transfer plan for $D(m)$, i. e., $\int d\pi(x_0, \,.\,) = m + 1$ and $\int d\pi(\,.\,, x_1) = 1$. We set

$$D_\pi = \iint c(|x_1 - x_0|)\, d\pi(x_0, x_1).$$

As a first step, we claim that for all φ smooth and $r > 0$ we can estimate

$$\left| \fint \varphi \, m \, dx \right| \leq r \sup |\nabla \varphi| + \frac{2D_\pi}{c(r)} \sup |\varphi|. \tag{26}$$

Indeed, since π is an admissible transfer plan we may write

$$\fint \varphi \, m \, dx \;=\; \fint \varphi \, ((m+1) - 1) \, dx \;=\; \iint (\varphi(x_1) - \varphi(x_0)) \, d\pi(x_0, x_1),$$

and furthermore,

$$\begin{aligned} \fint \varphi \, m \, dx \;&=\; \iint \chi_{\{|x_1 - x_0| \leq r\}} (\varphi(x_1) - \varphi(x_0)) \, d\pi(x_0, x_1) && (27) \\ &\quad + \iint \chi_{\{|x_1 - x_0| > r\}} (\varphi(x_1) - \varphi(x_0)) \, d\pi(x_0, x_1), && (28) \end{aligned}$$

The r. h. s. in (27) is estimated as follows

$$\begin{aligned} &\left| \iint \chi_{\{|x_1 - x_0| \leq r\}} (\varphi(x_1) - \varphi(x_0)) \, d\pi(x_0, x_1) \right| \\ &\quad \leq \; \sup |\nabla \varphi| \, r \iint \chi_{\{|x_1 - x_0| \leq r\}} d\pi(x_0, x_1) \\ &\quad \leq \; \sup |\nabla \varphi| \, r. \end{aligned}$$

For (28), we have

$$\begin{aligned} &\left| \iint \chi_{\{|x_1 - x_0| > r\}} (\varphi(x_1) - \varphi(x_0)) \, d\pi(x_0, x_1) \right| \\ &\quad \leq \; 2 \sup |\varphi| \iint \chi_{\{|x_1 - x_0| > r\}} d\pi(x_0, x_1) \\ &\quad \leq \; 2 \sup |\varphi| \frac{1}{c(r)} \iint \chi_{\{|x_1 - x_0| > r\}} c(|x_1 - x_0|) \, d\pi(x_0, x_1) \\ &\quad \leq \; 2 \sup |\varphi| \frac{1}{c(r)} D_\pi. \end{aligned}$$

For the second inequality, we have used the monotonicity of c. This proves (26).

In the following, C denotes a generic constant only depending on the space dimension d, whose value may change from line to line.

From (26) we infer that for all r, $R > 0$ we have

$$\fint m^2 \, dx \;\leq\; \left(C \frac{r}{R} + \frac{2D_\pi}{c(r)} + CR \fint |\nabla m| \, dx \right) \sup |m|. \tag{29}$$

For this purpose we select a smooth function $\zeta : \mathbb{R}^d \to [0, \infty)$ with $\operatorname{supp} \zeta \subset B_1(0)$ and $\int \zeta \, dx = 1$. We set $\zeta_R(x) = \frac{1}{R^d} \zeta(\frac{x}{R})$. We denote by m_R the convolution of m with ζ_R.

We use the convolution to split m, and accordingly the r. h. s. of (29):

$$\fint m^2\,dx \;=\; \fint m_R\,m\,dx + \fint (m-m_R)m\,dx.$$

We estimate the first term with the help of (26):

$$\begin{aligned}\left|\fint m_R\,m\,dx\right| &\le r\sup|\nabla m_R| + \frac{2D_\pi}{c(r)}\sup|m_R| \\ &\le r\frac{C}{R}\sup|m| + \frac{2D_\pi}{c(r)}\sup|m|.\end{aligned}$$

For the second term we have

$$\begin{aligned}\left|\fint (m-m_R)m\,dx\right| &\le \fint |m-m_R|\,dx\,\sup|m| \\ &\le CR\fint|\nabla m|\,dx\,\sup|m|.\end{aligned}$$

This proves (29).

Finally, we address the assertion, (21). Since $m\in\{-1,1\}$ by assumption in Proposition 3, (29) turns into

$$1 \;\le\; C\frac{r}{R} + \frac{2D_\pi}{c(r)} + CR\fint|\nabla m|\,dx.$$

We optimize in R by choosing $R = r^{1/2}\left(\fint|\nabla m|\,dx\right)^{-1/2}$, which yields

$$\frac{1}{2} \;\le\; Cr^{1/2}\left(\fint|\nabla m|\,dx\right)^{1/2} + \frac{D_\pi}{c(r)}.$$

We now choose r such that

$$Cr^{1/2}\left(\fint|\nabla m|\,dx\right)^{1/2} \;=\; \frac{1}{4}.$$

Then

$$c\left(\frac{1}{16C^2}\left(\fint|\nabla m|\,dx\right)^{-1}\right) \;\le 4D_\pi.$$

Minimizing in π yields (21).

□

The proof of Proposition 1 imitates closely the one of [15, Lemma 3].

Proof of Proposition 1 We introduce the notation $E(t) = E(m(t))$ and $D(t) = D(m(t))$. We treat the cases $D(T)\ge 2D(0)$ and $D(T) < 2D(0)$ separately. We first

turn to the "$\geq$"-case, and estimate with the help of the dissipation inequality (14) resp. (20):

$$\begin{aligned} D(T) - D(0) &\leq \int_0^T \frac{d^+}{dt} D \, dt \\ &\lesssim \int_0^T \left(-\frac{dE}{dt} \right)^{1/2} dt \\ &\leq \left(\int_0^T \left(-\frac{dE}{dt} \right) \frac{1}{E} \, dt \right)^{1/2} \left(\int_0^T E \, dt \right)^{1/2} \\ &= \left(\ln \frac{1}{E(T)} - \ln \frac{1}{E(0)} \right)^{1/2} \left(\int_0^T E \, dt \right)^{1/2}. \end{aligned}$$

Using $D(T) \geq 2D(0)$ and $E(0) \leq 1$ this becomes

$$\int_0^T E \, dt \gtrsim \frac{D(T)^2}{\ln \frac{1}{E(T)}}. \tag{30}$$

Thanks to the interpolation inequality (15) the r.h.s. in (30) is controlled by the energy:

$$\int_0^T E \, dt \gtrsim \ln \frac{1}{E(T)}.$$

Setting $h(T) = \int_0^T E \, dt$ this reads $h(T) \gtrsim \ln \frac{1}{h'(T)}$, so we have shown that

$$\frac{d}{dT} \left(\frac{1}{c_0} \exp(c_0 \, h(T)) \right) \geq 1 \qquad \text{provided } D(T) \geq 2D(0), \tag{31}$$

for some constant $c_0 > 0$.

Now we assume $D(T) < 2D(0)$. Then (15) implies

$$D(0) \gtrsim \ln \frac{1}{E(T)},$$

or in terms of h:

$$\exp(c_1 \, D(0)) \, h'(T) \geq 1 \qquad \text{provided } D(T) < 2D(0), \tag{32}$$

for some constant $c_1 > 0$. Combining (31) and (32) we conclude that

$$\frac{d}{dT} \left(\frac{1}{c_0} \exp(c_0 \, h(T)) + \exp(c_1 \, D(0)) \, h(T) \right) \geq 1.$$

Integration in time yields

$$\frac{1}{c_0} \exp(c_0 \, h(T)) + \exp(c_1 \, D(0)) \, h(T) \geq T,$$

and thus

$$\frac{2}{c_0}\exp(c_1\,D(0)+c_0\,h(T)) \;\geq\; T.$$

Finally, using $\ln T \gg D(0) \gtrsim 1$, this becomes

$$h(T) \;\gtrsim\; \ln T,$$

which is the assertion of Proposition 1.

□

Appendix A

In this appendix, we derive a useful formula for the rate of change of the Monge-Kantorowicz-Rubinstein distance in a situation, where the mass densities are transported by a smooth velocity field. We consider

$$\begin{aligned} &D(\rho_0,\rho_1)\\ &\quad= \inf\left\{ \iint c(|x_1-x_0|)\,d\pi(x_0,x_1)\;\Big|\; \int d\pi(\,.\,,x_1)=\rho_0,\ \int d\pi(x_0,\,.\,)=\rho_1\right\}, \end{aligned}$$

where ρ_0, ρ_1 are nonnegative densities such that $⨍\,\rho_i\,dx = 1$ for $i=0,1$, and c is a strictly concave, C^1 cost function. The condition on the transfer plan π means that π has marginals $\mathcal{L}^d\llcorner\rho_0$ and $\mathcal{L}^d\llcorner\rho_1$: $\pi[U\times[0,\Lambda]^d] = \mathcal{L}^d\llcorner\rho_0[U]$ and $\pi[[0,\Lambda]^d\times U] = \mathcal{L}^d\llcorner\rho_1[U]$ for each Borel set $U\subset[0,\Lambda]^d$.

The existence of an optimal transfer plan π_{opt} follows by a standard continuity-compactness argument. For strictly concave cost functions $c(z)$, π_{opt} is unique [12].

Lemma 1. *Let u be a smooth velocity field and ρ_0, ρ_1 two densities in $C([0,T];L^2_{per}(0,\Lambda)^d)$ for some $T>0$. Assume that*

$$\partial_t\,\rho_i + \nabla\cdot(\rho_i u) \;=\; 0, \tag{33}$$

for $i=0,1$. Then we have

$$\frac{d^+}{dt}D(\rho_0(t),\rho_1(t)) \;\leq\; \iint c'(|x_1-x_0|)\frac{x_1-x_0}{|x_1-x_0|}\cdot(u(t,x_1)-u(t,x_0))\,d\pi_{opt}(t)(x_0,x_1).$$

Proof of Lemma 1 We consider the flow ϕ_δ which is generated by $u(t+\,\cdot\,,\,\cdot\,)$, this means,

$$\partial_\delta\,\phi_\delta(x) \;=\; u(t+\delta,\phi_\delta(x)) \qquad\text{and}\qquad \phi_0(x) \;=\; x.$$

Then $\rho_i(t+\delta,\,\cdot\,)$ is the push-forward of $\rho_i(t,\,\cdot\,)$ under the flow ϕ_δ:

$$\int \zeta(x)\rho_i(t+\delta,x)\,dx \;=\; \int \zeta(\phi_\delta(x))\rho_i(t,x)\,dx, \qquad \text{for any periodic } \zeta.$$

This fact follows easily from (33). Consequently, the forward-pushed transfer plan $\pi_\delta(t) = \phi_\delta \# \pi_{opt}(t)$ defined by

$$\iint \zeta(x_0, x_1)\, d\pi_\delta(t)(x_0, x_1) \;=\; \iint \zeta(\phi_\delta(x_0), \phi_\delta(x_1))\, d\pi_{opt}(t)(x_0, x_1),$$

for any periodic ζ, is admissible as transfer plan $\pi(t+\delta)$. Therefore we may estimate

$$\begin{aligned}
&(D(\rho_0(t+\delta), \rho_1(t+\delta)) - D(\rho_0(t), \rho_1(t))) \\
&\leq \left(\iint c(|x_1 - x_0|)\, d\pi_\delta(t)(x_0, x_1) - \iint c(|x_1 - x_0|)\, d\pi_{opt}(t)(x_0, x_1) \right) \\
&= \iint \left(c(|\phi_\delta(x_1) - \phi_\delta(x_0)|) - c(|x_1 - x_0|) \right) d\pi_{opt}(t)(x_0, x_1),
\end{aligned}$$

which holds true for any $\delta > 0$. Thus

$$\frac{d^+}{dt} D(\rho_0(t), \rho_1(t)) \;\leq\; \iint \partial_{\delta|\delta=0}\, c(|\phi_\delta(x_1) - \phi_\delta(x_0)|)\, d\pi_{opt}(t)(x_0, x_1).$$

Finally, we compute

$$\partial_{\delta|\delta=0}\, c(|\phi_\delta(x_1) - \phi_\delta(x_0)|) \;=\; c'(|x_1 - x_0|) \frac{x_1 - x_0}{|x_1 - x_0|} \cdot (u(x_1) - u(x_0)),$$

which yields the assertion in Lemma 1.

□

Appendix B

In the proof of Proposition 2 we have used the notion of maximal functions. For a given locally integrable function f, its maximal function $M f$ is defined by

$$(M f)(x_0) \;=\; \sup_{r>0} \frac{1}{|B_r|} \int_{B_r(x_0)} f\, dx.$$

The following two lemmas can be found in [23]. For the convenience of the reader we present the proof of the first one.

Lemma 2. *The following estimate holds for a. e. x, y:*

$$|f(x) - f(y)| \;\lesssim |x - y|((M\,|\nabla f|)(x) + (M\,|\nabla f|)(y)).$$

Lemma 3. *For $1 < p < \infty$ we have:*

$$\int |M\, f|^p\, dx \;\lesssim\; \int |f|^p\, dx.$$

Proof of Lemma 2 For $x \neq y$ we let $R = \frac{1}{2}|x-y|$. Then we have

$$\frac{|f(x)-f(y)|}{|x-y|} \lesssim \frac{1}{R^{d+1}} \int_{B_R(x)} |f(x)-f(z)|\,dz + \frac{1}{R^{d+1}} \int_{B_R(y)} |f(y)-f(z)|\,dz.$$

It remains to show that

$$\frac{1}{R^{d+1}} \int_{B_R(x)} |f(x)-f(z)|\,dz \lesssim (M|\nabla f|)(x).$$

W. l. o. g. we may assume that $x = 0$. Indeed, we see easily:

$$\begin{aligned} \frac{1}{R^{d+1}} \int_{B_R(0)} |f(0)-f(z)|\,dz &\leq \frac{1}{R^{d+1}} \int_{B_R(0)} \int_0^1 |\nabla f(sz)||z|\,ds dz \\ &\leq \int_0^1 \frac{1}{R^d} \int_{B_R(0)} |\nabla f(sz)|\,dz ds \\ &\leq (M|\nabla f|)(0). \end{aligned}$$

In the last inequality we have used that

$$\sup_R \frac{1}{R^d} \int_{B_R(0)} |\nabla f(sz)|\,dz = \sup_R \frac{1}{R^d} \int_{B_R(0)} |\nabla f(z)|\,dz.$$

□

Acknowledgements

FO thanks for partial support by the DFG through the Hausdorff Center for Mathematics. CS was supported by the German Science Foundation through SFB 611. He thanks Patrick Penzler, Jutta Steiner, and Martin Zimmermann for fruitful discussions concerning numerical simulations.

References

[1] F. J. Alexander, S. Chen, and D. W. Grunau. Hydrodynamic spinodal decomposition: Growth kinetics and scaling functions. *Phys. Rev. B*, 48(1):634–637, Jul 1993.

[2] Luigi Ambrosio. Transport equation and Cauchy problem for non-smooth vector fields. In *Calculus of variations and nonlinear partial differential equations*, volume 1927 of *Lecture Notes in Math.*, pages 1–41. Springer, Berlin, 2008.

[3] Alan J. Bray. Theory of phase-ordering kinetics. *Advances in Physics*, 51(2):481– 587, 2002.

[4] Alberto Bressan. A lemma and a conjecture on the cost of rearrangements. *Rend. Sem. Mat. Univ. Padova*, 110:97–102, 2003.

[5] Y. C. Chou and Walter I. Goldburg. Phase separation and coalescence in critically quenched isobutyric-acid¯water and 2,6-lutidine¯water mixtures. *Phys. Rev. A*, 20(5):2105–2113, Nov 1979.

[6] Sergio Conti, Barbara Niethammer, and Felix Otto. Coarsening rates in off-critical mixtures. *SIAM J. Math. Anal.*, 37(6):1732–1741 (electronic), 2006.

[7] Gianluca Crippa and Camillo De Lellis. Estimates and regularity results for the DiPerna-Lions flow. *J. Reine Angew. Math.*, 616:15–46, 2008.

[8] Shibin Dai and Robert L. Pego. Universal bounds on coarsening rates for mean-field models of phase transitions. *SIAM J. Math. Anal.*, 37(2):347–371 (electronic), 2005.

[9] Shibin Dai and Robert L. Pego. An upper bound on the coarsening rate for mushy zones in a phase-field model. *Interfaces Free Bound.*, 7(2):187–197, 2005.

[10] Selim Esedoḡlu and John B. Greer. Upper bounds on the coarsening rate of discrete, ill-posed nonlinear diffusion equations. *Comm. Pure Appl. Math.*, 62(1):57–81, 2009.

[11] Selim Esedoḡlu and Dejan Slepčev. Refined upper bounds on the coarsening rate of discrete, ill-posed diffusion equations. *Nonlinearity*, 21(12):2759–2776, 2008.

[12] Wilfrid Gangbo and Robert J. McCann. The geometry of optimal transportation. *Acta Math.*, 177(2):113–161, 1996.

[13] K. B. Glasner and T. P. Witelski. Coarsening dynamics of dewetting films. *Physical Review E (Statistical, Nonlinear, and Soft Matter Physics)*, 67(1):016302, 2003.

[14] T. Koga and K. Kawasaki. Late stage dynamics of spinodal decomposition in binary fluid mixtures. *Physica A Statistical Mechanics and its Applications*, 196:389–415, June 1993.

[15] Robert V. Kohn and Felix Otto. Upper bounds on coarsening rates. *Comm. Math. Phys.*, 229(3):375–395, 2002.

[16] Robert V. Kohn and Xiaodong Yan. Upper bound on the coarsening rate for an epitaxial growth model. *Comm. Pure Appl. Math.*, 56(11):1549–1564, 2003.

[17] Robert V. Kohn and Xiaodong Yan. Coarsening rates for models of multicomponent phase separation. *Interfaces Free Bound.*, 6(1):135–149, 2004.

[18] Felix Otto, Tobias Rump, and Dejan Slepčev. Coarsening rates for a droplet model: rigorous upper bounds. *SIAM J. Math. Anal.*, 38(2):503–529 (electronic), 2006.

[19] Sanjay Puri and Burkhard Dünweg. Temporally linear domain growth in the segregation of binary fluids. *Phys. Rev. A*, 45(10):R6977–R6980, May 1992.

[20] Lorenz Ratke and Peter W. Voorhes. *Growth and Coarsening. Ripening in Material Processing*. Springer, 2002.

[21] Eric D. Siggia. Late stages of spinodal decomposition in binary mixtures. *Phys. Rev. A*, 20(2):595–605, Aug 1979.

[22] Dejan Slepčev. Coarsening in nonlocal interfacial systems. *SIAM J. Math. Anal.*, 40(3):1029–1048, 2008.

[23] Elias M. Stein. *Singular integrals and differentiability properties of functions*. Princeton Mathematical Series, No. 30. Princeton University Press, Princeton, N.J., 1970.

[24] Oriol T. Valls and James E. Farrell. Spinodal decomposition in a three-dimensional fluid model. *Phys. Rev. E*, 47(1):R36–R39, Jan 1993.

[25] Cédric Villani. *Topics in optimal transportation*, volume 58 of *Graduate Studies in Mathematics*. American Mathematical Society, Providence, RI, 2003.

[26] Cédric Villani. *Optimal transport. Old and new*, volume 338 of *Grundlehren der Mathematischen Wissenschaften [Fundamental Principles of Mathematical Sciences]*. Springer-Verlag, Berlin, 2009.

[27] N.-C. Wong and C. M. Knobler. Light scattering studies of phase separation in isobutyric acid + water mixtures. *J. chem. Phys.*, 69:725–735, jul 1978.

[28] Ning-Chih Wong and Charles M. Knobler. Light-scattering studies of phase separation in isobutyric acid + water mixtures: Hydrodynamic effects. *Phys. Rev. A*, 24(6):3205–3211, Dec 1981.

Bestellungen nimmt entgegen:

Sonderforschungsbereich 611
der Universität Bonn
Poppelsdorfer Allee 82
D - 53115 Bonn

Telefon: 0228/73 4882
Telefax: 0228/73 7864
E-Mail: astrid.link@ins.uni-bonn.de http://www.sfb611.iam.uni-bonn.de/

Verzeichnis der erschienenen Preprints ab No. 430

430. Frehse, Jens; Málek, Josef; Ružička, Michael: Large Data Existence Result for Unsteady Flows of Inhomogeneous Heat-Conducting Incompressible Fluids

431. Croce, Roberto; Griebel, Michael; Schweitzer, Marc Alexander: Numerical Simulation of Bubble and Droplet Deformation by a Level Set Approach with Surface Tension in Three Dimensions

432. Frehse, Jens; Löbach, Dominique: Regularity Results for Three Dimensional Isotropic and Kinematic Hardening Including Boundary Differentiability

433. Arguin, Louis-Pierre; Kistler, Nicola: Small Perturbations of a Spin Glass System

434. Bolthausen, Erwin; Kistler, Nicola: On a Nonhierarchical Version of the Generalized Random Energy Model. II. Ultrametricity

435. Blum, Heribert; Frehse, Jens: Boundary Differentiability for the Solution to Hencky's Law of Elastic Plastic Plane Stress

436. Albeverio, Sergio; Ayupov, Shavkat A.; Kudaybergenov, Karim K.; Nurjanov, Berdach O.: Local Derivations on Algebras of Measurable Operators

437. Bartels, Sören; Dolzmann, Georg; Nochetto, Ricardo H.: A Finite Element Scheme for the Evolution of Orientational Order in Fluid Membranes

438. Bartels, Sören: Numerical Analysis of a Finite Element Scheme for the Approximation of Harmonic Maps into Surfaces

439. Bartels, Sören; Müller, Rüdiger: Error Controlled Local Resolution of Evolving Interfaces for Generalized Cahn-Hilliard Equations

440. Bock, Martin; Tyagi, Amit Kumar; Kreft, Jan-Ulrich; Alt, Wolfgang: Generalized Voronoi Tessellation as a Model of Two-dimensional Cell Tissue Dynamics

441. Frehse, Jens; Specovius-Neugebauer, Maria: Existence of Hölder Continuous Young Measure Solutions to Coercive Non-Monotone Parabolic Systems in Two Space Dimensions

442. Kurzke, Matthias; Spirn, Daniel: Quantitative Equipartition of the Ginzburg-Landau Energy with Applications

443. Bulíček, Miroslav; Frehse, Jens; Málek, Josef: On Boundary Regularity for the Stress in Problems of Linearized Elasto-Plasticity

444. Otto, Felix; Ramos, Fabio: Universal Bounds for the Littlewood-Paley First-Order Moments of the 3D Navier-Stokes Equations

445. Frehse, Jens; Specovius-Neugebauer, Maria: Existence of Regular Solutions to a Class of Parabolic Systems in Two Space Dimensions with Critical Growth Behaviour

446. Bartels, Sören; Müller, Rüdiger: Optimal and Robust A Posteriori Error Estimates in $L^\infty(L^2)$ for the Approximation of Allen-Cahn Equations Past Singularities

447. Bartels, Sören; Müller, Rüdiger; Ortner, Christoph: Robust A Priori and A Posteriori Error Analysis for the Approximation of Allen-Cahn and Ginzburg-Landau Equations Past Topological Changes

448. Gloria, Antoine; Otto, Felix: An Optimal Variance Estimate in Stochastic Homogenization of Discrete Elliptic Equations

449. Kurzke, Matthias; Melcher, Christof; Moser, Roger; Spirn, Daniel: Ginzburg-Landau Vortices Driven by the Landau-Lifshitz-Gilbert Equation

450. Kurzke, Matthias; Spirn, Daniel: Gamma-Stability and Vortex Motion in Type II Superconductors

451. Conti, Sergio; Dolzmann, Georg; Müller, Stefan: The Div–Curl Lemma for Sequences whose Divergence and Curl are Compact in $W^{-1,1}$

452. Barret, Florent; Bovier, Anton; Méléard, Sylvie: Uniform Estimates for Metastable Transition Times in a Coupled Bistable System

453. Bebendorf, Mario: Adaptive Cross Approximation of Multivariate Functions

454. Albeverio, Sergio; Hryniv, Rostyslav; Mykytyuk, Yaroslav: Scattering Theory for Schrödinger Operators with Bessel-Type Potentials

455. Weber, Hendrik: Sharp Interface Limit for Invariant Measures of a Stochastic Allen-Cahn Equation

456. Harbrecht, Helmut: Finite Element Based Second Moment Analysis for Elliptic Problems in Stochastic Domains

457. Harbrecht, Helmut; Schneider, Reinhold: On Error Estimation in Finite Element Methods without Having Galerkin Orthogonality

458. Albeverio, S.; Ayupov, Sh. A.; Rakhimov, A. A.; Dadakhodjaev, R. A.: Index for Finite Real Factors

459. Albeverio, Sergio; Pratsiovytyi, Mykola; Pratsiovyta, Iryna; Torbin, Grygoriy: On Bernoulli Convolutions Generated by Second Ostrogradsky Series and their Fine Fractal Properties

460. Brenier, Yann; Otto, Felix; Seis, Christian: Upper Bounds on Coarsening Rates in Demixing Binary Viscous Liquids